Dynamic alternations of RANKL/OPG ratio expressed by cementocytes in response to orthodontic-induced external apical root resorption in a rat model

TINGTING WEI[1,2], ZHIYI SHAN[3], XIN WEN[2], NING ZHAO[2] and GANG SHEN[2]

Departments of [1]Preventive Dentistry and [2]Orthodontics, Shanghai Key Laboratory of Stomatology, Shanghai Ninth People's Hospital, College of Stomatology, Shanghai Jiao Tong University School of Medicine, Shanghai 200011; [3]Department of Orthodontics, Faculty of Dentistry, The University of Hong Kong, Hong Kong, SAR, P.R. China

Received February 12, 2022; Accepted May 5, 2022

DOI: 10.3892/mmr.2022.12744

Abstract. The aim of the present study was to investigate the alterations in the formation of cementocytes in response to orthodontic forces and to evaluate the contribution of these cells in the biological changes of tooth movement and associated root resorption. A total of 90 Sprague Dawley rats were randomly assigned to the control, high force, and low force groups. Intrusion forces of 10 and 50 g were applied on the rat molar to induce tooth intrusion. The tooth movement was observed from 0 to 14 days by micro-computed tomography, bone histometric analysis, tartrate-resistant acid phosphatase staining, as well as reverse transcription-quantitative PCR and immunofluorescence staining assays. The results suggested that under low force conditions, osteoclasts were distributed at a higher frequency on the bone side than on the root side. Under high force conditions, both sides suffered osteoclast infiltration. In the low force group, the cementocytes exhibited downregulated sclerostin (*SOST*) and osteoprotegerin (*OPG*) mRNA levels and a lower receptor activator of nuclear factor-κB ligand (*RANKL*)/*OPG* ratio over a certain period of time. The expression levels of these genes were lower compared with those of the osteocytes at each time-point. In the high force group, both cementocytes and osteocytes upregulated the *SOST* and *RANKL*/*OPG* ratio on days 7 and 14, while the cementocytes expressed higher levels of *SOST* mRNA than those noted in the osteocytes. These data suggested that cementocytes responded to the orthodontic force via modulation of the *RANKL*/*OPG* ratio and *SOST* expression. The biological response of cementocytes contributed to the mechanotransduction and homoeostasis of the roots under compression. Excessive forces may act as a negative factor of this regulatory role. These results expand our knowledge on the function of cementocytes.

Introduction

The side effects of orthodontic tooth movement include orthodontic-induced external apical root resorption (EARR), periodontal inflammation, and tooth demineralization and loosening, among which EARR is the most common side effect (1). The mechanical factors noted in specific treatment techniques, such as the duration of force application and force magnitude and direction, are associated with the degree of EARR (2,3). It has been shown that periodontal ligament cells (PDLc), which are compressed by forces applied on teeth, secrete osteoclastogenic cytokines to stimulate bone resorption in the direction of the orthodontic force vector (4). EARR is associated with the cellular activity of over-compressed PDLc and cementum resorption (5).

In contrast to these findings, recent studies have shown an alternative consideration regarding the role of cementocytes in the mechanotransduction and in the biological response during tooth movement. A previous *ex vivo* study by the authors indicated that cementocytes were sensitive to mechanical loading via the upregulation of sclerostin (*SOST*) expression, the increase in the receptor activator of nuclear factor-κB ligand (*RANKL*)/osteoprotegerin (*OPG*) ratio, and the downregulation of the expression levels of osteocalcin (6). Lira Dos Santos *et al* (7) demonstrated that cementocytes exhibited increased nuclear size and proportion of euchromatin under orthodontic loading, and reported a significant downregulation in the expression levels of type IV collagen

Correspondence to: Dr Gang Shen or Dr Ning Zhao, Department of Orthodontics, Shanghai Key Laboratory of Stomatology, Shanghai Ninth People's Hospital, College of Stomatology, Shanghai Jiao Tong University School of Medicine, 500 Quxi Road, Shanghai 200011, P.R. China
E-mail: shengang@bybo.com.cn
E-mail: zhaon1995@126.com

Abbreviations: EARR, external apical root resorption; RANKL, receptor of receptor activator of nuclear factor-κB ligand; μ-CT, micro-computed tomography; TRAP, tartrate-resistant acid phosphatase; RT-qPCR, reverse transcription-quantitative PCR; BV/TV, bone volume to tissue volume

Key words: cementocytes, cementum, orthodontic-induced external apical root resorption, osteoprotegerin, receptor activator of nuclear factor-κB ligand, sclerostin

following orthodontic tooth movement. In addition, cementocytes are also involved in cellular cementum apposition in mice and are associated with changes in cellular ultrastructure and in the proteomic profile of the cementum (8). These findings indicate that similar to PDLc, cementocytes play important roles in the biological events of the orthodontic tooth movement and the associated EARR.

Heavy and prolonged forces induce over-compression of PDLc and consequent cementum resorption, as aforementioned. However, the effect of force magnitude on cementocytes remains largely unknown. In the present study, the response of cementocytes was examined with regard to the intrusion forces of different magnitudes, and the variations in the expression levels of *RANKL/OPG*, and *SOST* were assessed in cementocytes grown under orthodontic forces.

A variety of signaling pathways and cytokines have been shown to be associated with tooth movement (9). The key regulators among them include the SOST, OPG, and RANKL proteins, which are capable of regulating the balance of osteoclastogenic and osteogenic differentiation (10). Previous *in vitro* studies have detected these gene expression profiles in cementocytes (6,11,12); therefore, in the present study, it was hypothesized that cementocytes may respond to the *in vivo* orthodontic force via regulation of expression of these genes.

The aim of the present study was to investigate the regulatory roles of cementocytes in the biological response to orthodontic intrusion forces, evaluate their contributions to the microenvironment homeostasis, and clarify the effect of force magnitude on the cementocyte behavior during orthodontic tooth intrusion.

Materials and methods

Intrusion loading in a rat model. The animal experiments were approved by the Animal Ethics Committee of Shanghai Ninth People's Hospital (approval no. SH9H-2020-A298-1) and the protocols were performed in accordance with the corresponding guidelines. Sprague Dawley rats (n=90; eight weeks old; weight, 289.1±37.21 g; 45 males and 45 females of specific pathogen-free grade) were randomly assigned to three groups as follows: Control group (n=30), low force group (n=30), and high force group (n=30). They were housed at 22±2˚C at 40-80% humidity and under a 12-h light/dark cycle with commercial feed and water *ad libitum*. Following anesthesia (1% pentobarbital sodium; 50 mg/kg body weight; intraperitoneal injection), a sterilized stainless-steel screw (1 mm in diameter and 4 mm in length) was implanted in the left palatal bone as an anchorage for loading. A sterilized 0.016x0.022 inch stainless steel wire (3M Unitek), which was bent into a specially designed 'L' loop was fixed between the screw and right maxillary first molar, followed by resin adhesion. The elasticity of the wire was adjusted by the length of the buckling part and the subsequent compressive force was adjusted to 10 g (low force group) and 50 g (high force group) using a dynamometer. The rats in the control group received a resin adhesion without intrusion force loading. None of the intrusion appliances were removed during treatment. At each time-point, the rats were sacrificed by overdose of anesthesia (1% pentobarbital sodium; 100 mg/kg body weight; intraperitoneal injection) and cervical dislocation if needed, and their vital signs were confirmed by heartbeat and pupillary response to light, following the American Veterinary Medical Association guidelines (13). The left first molar and the surrounding alveolar bone were harvested.

Micro-computed tomography (μ-CT) scanning. A total of 45 rats were randomly selected in each group for μ-CT scanning. Three rats were randomly selected each on days 1, 2, 4, 7 and 14. Their samples were fixed in 70% ethanol for 48 h at room temperature and scanned by a high-solution μ-CT (Scanco Medical AG). The following conditions were used: Resolution of 10 μm voxel size, voltage of 45 kV, current of 177 μA, and integration time of 200 msec. The data were reconstructed and the serial images were generated using the supporting analyzing software provided by the manufacturer. The distance of tooth movement was calculated as previously described (14,15). In short, the tooth movement was defined by the movement of the mesial buccal occlusal tip of the right maxillary first molar, and was measured by the deviation of the tip from the occlusal plane.

Bone histometric analysis. The quantitative analysis of the alveolar bone changes was conducted using serial images. The region of interest was set as a square area located in the intra-root alveolar bone of the right maxillary first molar, as previously described (15). The superior boundary was defined as the inferior plane of the root furcation. The transverse boundaries extended distally by the distal buccal root and mesially by the mesial root of the right maxillary first molar. Bone volume to tissue volume (BV/TV, 100%), bone mineral density (g/cm^3), trabecular number (per mm), trabecular thickness (μm), and trabecular separation (mm) were analyzed within the region.

Tartrate-resistant acid phosphatase (TRAP) staining. The samples were fixed in 4% paraformaldehyde for 48 h at room temperature, decalcified in 14% EDTA (pH 7.1) for 8 weeks, dehydrated and embedded in paraffin. The specimens were cut into 4-μm sections along the sagittal axis of the right maxillary first molar. For TRAP staining, deparaffinized sections were treated by an acid phosphatase kit (cat. no. 387A-1KT; MilliporeSigma) for 1 h in a 37˚C water bath protected from light, according to the manufacturer's instructions and counterstained 2 min at room temperature using Harris' hematoxylin solution. Images were obtained with an Olympus light microscope system (Olympus Corporation) at an objective magnification of x200. The region of interest (ROI) used for TRAP-positive cell quantification was located on the apex of the mesial root (600 μm width and 400 μm length). The contour of the cellular cementum and corresponding alveolar bone in this region were depicted. Osteoclast cells, which were TRAP-positive multinucleated cells near the linear surfaces of the cellular cementum and alveolar bone, were quantified separately. The data were normalized as the mean number of cells per millimeter of cellular cementum and alveolar bone surface. The root resorption of the mesial root of the first molar at each time-point was evaluated by root resorption scores as previously described (16). In short, the ROI on the magnified (x200) image was divided into 10x10 mm grids. Root resorption scores were determined by dividing the number of grids

Table I. List of primer sequences used in reverse transcription-quantitative PCR.

Gene	Forward primer (5'-3')	Reverse primer (5'-3')
GAPDH	TGATGGGTGTGAACCACGAG	TACTTGGCAGGTTTCTCCAGG
OPG	TGTCCGGATGGGTTCTTCTCA	GCACAGGGTGACATCTATTCCA
RANKL	CAGCATCGCTCTGTTCCTGTA	CTGCGTTTTCATGGAGTCTCA
SOST	TACATGCAGCCTTCGTTGCT	CTCGGACACGTCTTTGGTGT

OPG, osteoprotegerin; *RANKL*, receptor activator of nuclear factor-kB; *SOST*, sclerostin.

with resorption lacunae by the total number of grids along the root surface.

Immunohistochemical staining. Paraffin-embedded tissue sections were used following deparaffinization with xylene and rehydration through a series of experimental steps, including alcohol washes, 0.5% pepsin antigen retrieval, and blocking steps (10% hydrogen peroxide for 15 min at room temperature to quench endogenous peroxidase activity and 10% normal donkey serum for 30 min at 4˚C to block non-specific binding). The primary antibodies were polyclonal rabbit anti-OPG (1:400; cat. no. 183910; Abcam) and monoclonal mouse anti-RANKL (1:100; cat. no. sc-52950; Santa Cruz Biotechnology, Inc.). The primary antibody was omitted in the negative control and no labeling was observed in any case. Donkey anti-rabbit and anti-mouse secondary antibodies (Jackson Immuno Research, Inc.) were used respectively at 1:200 dilutions. Following incubation with the primary antibodies at 4˚C overnight, secondary antibodies were used respectively at 1:200 dilutions for 2 h at room temperature. Sections were incubated using a DAB substrate kit (Thermo Fisher Scientific, Inc.) for 2 min at room temperature and then counterstained with Harris' hematoxylin (for RANKL, 2 min, room temperature) or 0.5% methyl green (for OPG, 1 min, room temperature). Images were obtained with an Olympus light microscope system (Olympus Corporation) at an objective magnification of x200.

Immunofluorescence staining. Paraffin-embedded tissue sections were treated the same way as the sections used for immunohistochemical staining. The primary antibody was a polyclonal goat anti-SOST (cat. no. AF1589; R&D Systems, Inc.) used at 1:50 dilutions. PBS was used as the control antibody in the negative control sample. Donkey anti-goat Alexa Fluor secondary antibody (cat. no. A-11058; Invitrogen; Thermo Fisher Scientific, Inc.) was used at a 1:200 dilution. Following incubation with the primary antibodies at 4˚C overnight, the secondary antibody was used respectively at 1:200 dilutions for 2 h at room temperature. The sections were subsequently stained with 1 μg/ml DAPI for 10 min at 4˚C (Invitrogen; Thermo Fisher Scientific, Inc.). The images were obtained using an Olympus fluorescence microscope system (Olympus Corporation) at a magnification of x400. Image-Pro Plus version 6.0 software (Media Cybernetics, Inc.) was used to assess the integrated optical density (IOD) value and area of the section. Three random fields from the cellular cementum and the surrounding alveolar bone were selected separately to calculate the mean density of each area.

Reverse transcription-quantitative PCR (RT-qPCR). To quantitatively compare the gene expression levels of the cementocytes and osteocytes following orthodontic intrusion, the cellular cementum and the alveolar bone were separately collected using a previously described method (17). A total of 15 rats in each group were sacrificed to collect samples for RT-qPCR. Three rats were randomly selected for each time-point (n=3). Briefly, the cementum was detached from the apical region of the mesial root of the intruded molar and the alveolar bone was isolated from the periapical area of the same root. The tissues were dissected in three cycles of serial digestion with collagenase A (300 U/l; MilliporeSigma) and EDTA (5 mM, in 0.1% bovine serum albumin; MilliporeSigma) for 20 min each at 37˚C for elimination of periodontal contamination. Total RNA was extracted from each digested sample using a MiniBEST Universal RNA Extraction kit (cat. no. 9767; Takara Bio, Inc.) according to the manufacturer's instructions. The RNA samples were reverse transcribed to cDNA using a PrimeScript RT reagent Kit (cat. no. RR036A; Takara Bio, Inc.) according to the manufacturer's instructions. SYBR Premix Ex Taq (cat. no. RR420A; Takara Bio, Inc.) was used as a probe. The $2^{-\Delta\Delta Cq}$ method was used to estimate the relative RNA levels, which were normalized to those of *GAPDH*, as previously described (18). The primers were synthesized (Shanghai Sangong Pharmaceutical Co., Ltd.) and the sequences are shown in Table I.

Statistical analysis. Data are presented as the mean ± SEM. The data used for each parameter from μ-CT, TRAP staining, and RT-qPCR were analyzed and compared using SPSS 17.0 software (SPSS, Inc.). Multiple groups were compared using one-way ANOVA, followed by Bonferroni post hoc test to measure variances, while comparisons between two groups comparisons were performed using an unpaired Student's t-test. $P<0.05$ was considered to indicate a statistically significant difference.

Results

Orthodontic forces induce tooth intrusion and alveolar bone remodeling. To investigate the effects of the intrusion force on the tooth and alveolar bone, a tooth intrusion model was established. The forces applied were controlled by the wire length and measured using a force dynamometer (Fig. 1).

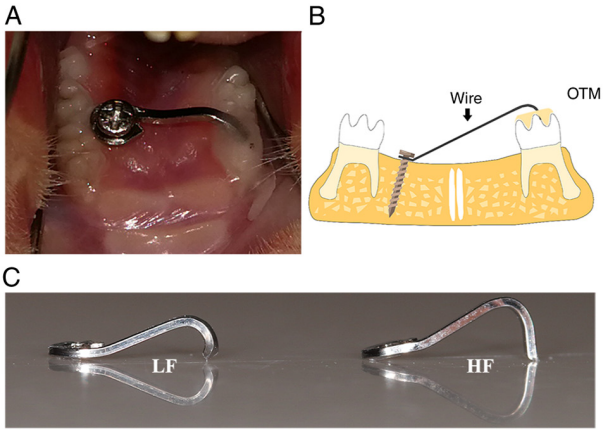

Figure 1. Right maxillary first molar intrusion model. The molar intrusion model is shown (A) occlusally and (B) transversally. A sterilized stainless-steel screw was implanted in the left palatal bone as a skeletal anchorage for intrusion. A sterilized stainless-steel wire which was bent into a special designed 'L' loop was fixed between the screw and the right maxillary first molar, followed by resin adhesion. The length of the buckling part was adjustable. When the wire was inserted, a dynamometer was used to measure the force applied to the tooth. (C) The intrusion force was adjusted to 10 g (LF) and 50 g (HF). LF, low force; HF, high force; OTM, orthodontic tooth movement.

The measurements of the forces were 9.12±1.37 g in the low force group and 54.97±4.10 g in the high force group. No significant differences were noted with regard to these parameters between male and female subjects (P>0.05; data not shown). A significant increase in tooth movement was detected in the low force group from day 1 to 7 (P<0.01); on day 14, tooth movement was not significantly increased compared with that of day 7 (P>0.05). In the high force group, the tooth movement was accelerated on day 4 (340.04±43.42 μm), which was significantly higher than that noted on day 1 (P<0.05). No significant increase was noted on day 7 compared with day 4, and on day 14 compared with day 7 (P>0.05). No significant difference was noted in the tooth movement between the low and high force groups detected at the time-points examined in the study (P>0.05). Quantitative bone histometric analysis revealed the significant differences noted between each group in the following parameters: BV/TV, bone mineral density, and trabecular numbers (P<0.05). The values of these parameters were reduced in the low force group compared with those noted in the control group, and were even lower in the high force group. The trabecular was significantly separated in both the low and high force groups compared with the control group (P<0.001); however, no significant difference was noted within them. In addition, the craters were observed in the alveolar bone in the high force group (Fig. 2).

Osteoclast formation is induced by compressive force. The resorption of the cellular cementum was detected under high force loading (Fig. 3). To evaluate the difference of osteoclast formation on the surface of the cellular cementum with the alveolar bone, the number of TRAP-positive osteoclasts on either side were quantified (Fig. 3). On the bone side, a significant increase in osteoclast numbers was detected after 6 h (low force, 6.77±1.07 cells/mm; high force, 5.63±1.11 cells/mm; P<0.01), and the number continued to increase over time. No significant differences were noted between the low and high force groups at any time-point. On the cementum side, the osteoclast number was significantly increased in the high force group at 24 h (5.18±0.65 cells/mm; P<0.01), but not in the low force group (0.57±0.49 cells/mm; P>0.05). Therefore, the number of osteoclasts on the cementum side of the high force group was considerably higher than that of the low force group when comparing between 24 h and 14 days (P<0.01). The number of osteoclasts was significantly higher on the bone side compared with that noted on the cementum side in the low force group when comparing between 6 h and 14 days (P<0.05). In the high force group, the differences were noted at 6 h (P<0.01), 24 h (P<0.05), and 14 days (P<0.05), when the bone side significantly surpassed the cementum side. As for the root resorption scores, significant increases were detected after 24 h in the high force group (P<0.01), but after 7 days in the low force group (P<0.05). From 24 h to 14 days, the root resorption scores of the high force group were significantly higher than those of the low force group (P<0.05).

Gene expression in the cellular cementum and the alveolar bone under compression. To investigate the role of cementocyte mechanotransduction during tooth intrusion, the cellular cementum mRNA expression profiles of *OPG, RANKL* and *SOST* were assessed. The surrounding alveolar bone was used for comparison (Fig. 4). In the low force group, the expression levels of *SOST* in both the cellular cementum and the alveolar bone were evaluated over time. The results indicated increased and decreased expression patterns. The expression levels in the cellular cementum were slightly increased at 24 h (1.26±0.56; P>0.05) and significantly decreased on day 7 compared with those of the control group (0.02±0.02; P<0.01). The expression levels of *SOST* mRNA in the bone side were significantly increased from 24 h (3.81±0.59; P<0.01) to 4 days (3.75±0.89, P<0.01) compared with those noted on day 0. From day 7 to day 14, the expression levels were significantly reduced. From 24 h to 14 days, the alveolar bone expressed significantly higher levels of *SOST* mRNA than those of the cellular cementum. In the high force group, the difference in the expression levels of *SOST* between the cellular cementum and the alveolar bone was only noted on days 4 and 7. At these time-points, *SOST* expression levels were significantly higher in the cellular cementum than those noted in the alveolar bone, indicating opposite findings to those noted at the same time-points in the low force group.

The expression levels of *OPG* were significantly increased in the cellular cementum on days 4 (5.31±0.35), 7 (5.10±0.13), and 14 (4.20±0.31) in the low force group, while in the high force group, the expression levels were reduced over time. In addition, the expression levels in the alveolar bone were significantly decreased from days 7 to 14 compared with those of day 0 in both low and high force groups. Significant differences between the cellular cementum and the alveolar bone were only noted in the low force group on days 4, 7 and 14 (P<0.01). The cellular cementum expressed approximately 8.67-(day 4), 16.29-(day 7), and 10.22-(day 14) fold higher levels of *OPG* than those noted in the alveolar bone. Immunohistochemistry identified intense OPG immunolocalization in the cellular cementum and cementocyte-like cells on day 14 in the low force group, while the alveolar bone OPG

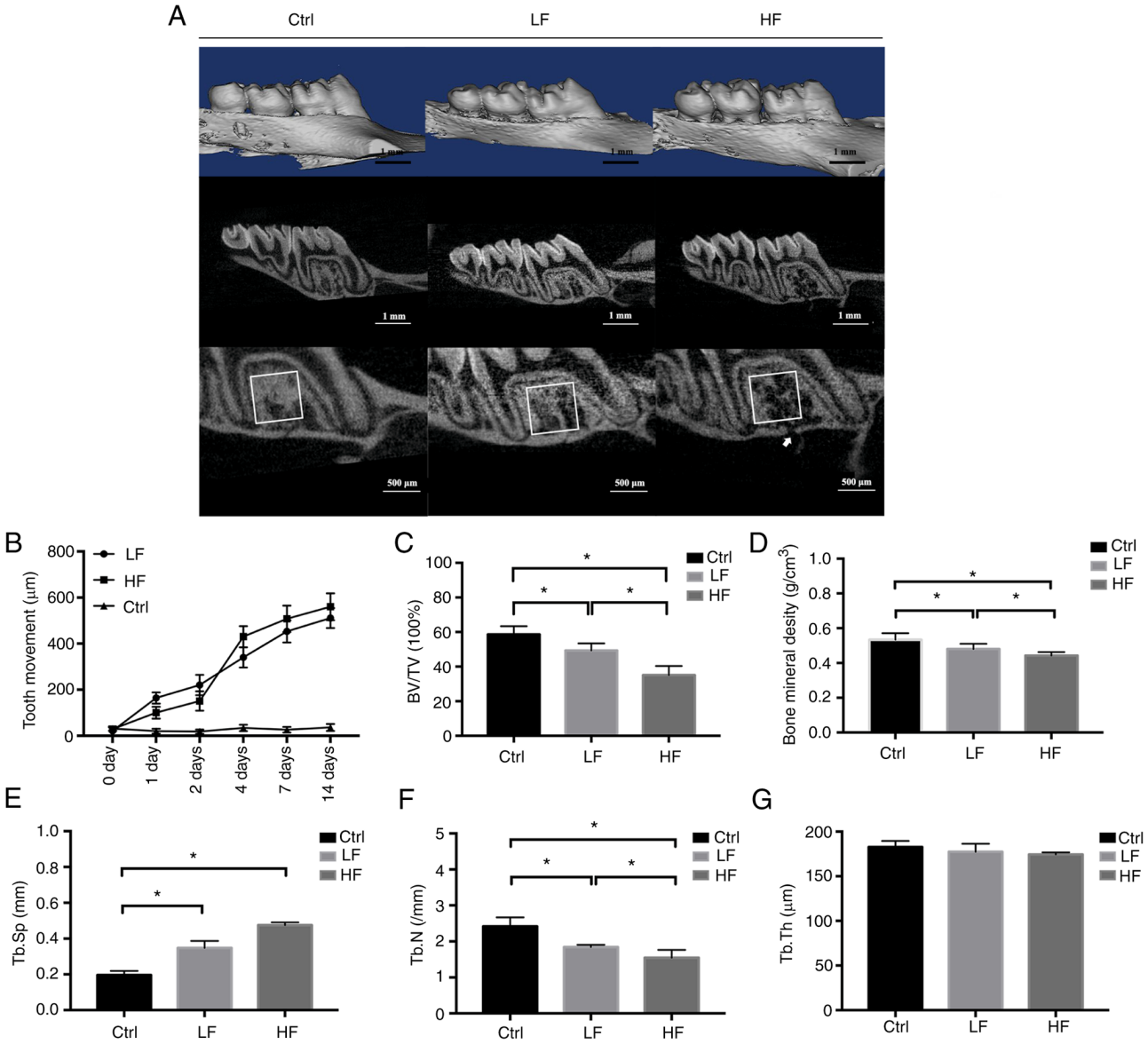

Figure 2. μ-CT images and bone histometric analysis. (A) The μ-CT scan and the reconstruction of the experimental maxillary in Ctrl, LF, and HF groups on day 14. A ROI was indicated by a square area located in the intra-root alveolar bone of right maxillary first molar. Histometric analysis was conducted with the ROI in each group. The white arrow indicated a small crater on the alveolar bone induced by loading. (B) Linear measurements of the experimental tooth movement. Data were presented by the distance of the tip from the occlusal plane (μm) over time. (C) BV/TV measured within the ROI in the Ctrl, LF and HF groups on day 14. (D) Bone mineral density analysis on day 14. (E) Tb.Sp on day 14. (F) Tb.N analysis on day 14. (G) Tb.Th on day 14. *P<0.05. μ-CT, micro-computed tomography; ROI, region of interest; BV/TV, bone volume to tissue volume; Ctrl, control; LF, low force; HF, high force; Tb.Sp, trabecular separation; Tb.N, trabecular number; Tb.Th, trabecular thickness.

labeling was similar. In the high force group, OPG labeling in both cellular cementum and alveolar bone was not found.

RANKL expression was elevated in the alveolar bone in the low force group from 6 h to 4 days and decreased thereafter. Upregulation of *RANKL* expression was noted in the cellular cementum on day 4 (1.40±0.66). Its expression levels were significantly lower than those of the alveolar bone (3.53±0.14) at the same time-point (P<0.05). In the low force group, the expression levels of the alveolar bone were significantly higher than those of the cellular cementum at every time-point observed. In the high force group, *RANKL* expression in both cementum and alveolar side was not significantly elevated with time from 0 to 24 h. Furthermore, the expression in the alveolar bone side was significantly higher than in the cementum side at these time-points (0 to 24 h). However, on day 4, *RANKL* expression in the cellular cementum surpassed that of the alveolar bone (1.91±0.21 compared with 1.45±0.29; P<0.05). Intense RANKL immunolocalization was found in both cementum and alveolar bone after 14 days of compression, either in the low force group and high force group. In the high force group, the periodontal ligament RANKL labeling was also detected.

In the low force group, the *RANKL*/*OPG* ratio in the cementum decreased over time and it was significantly lower than that of the bone from the time period between 24 h and 14 days. Moreover, the ratio of the alveolar bone was increased over time and peaked on day 7. In contrast to these findings, in the high force group, both the cellular cementum and the

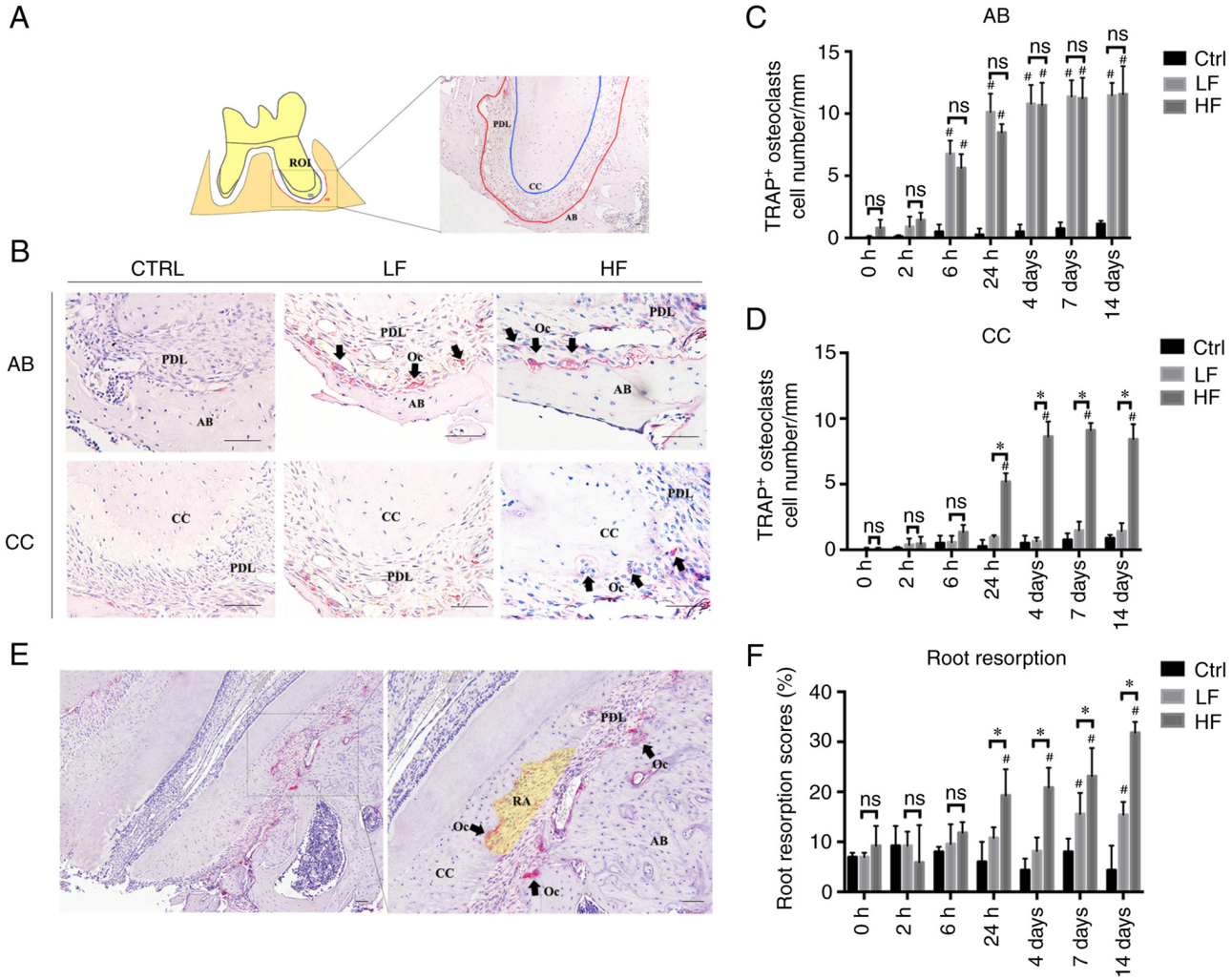

Figure 3. TRAP staining and osteoclast quantification. (A) Illustration of the apical area of the intruded molar. The ROI was 600 μm in width and 400 μm in length. The contour of CC (blue) and corresponding AB (red) are depicted. (B) The TRAP staining of CC and AB in the Ctrl, LF and HF groups on day 14. The TRAP-positive osteoclasts (black arrows) were stained in red. (C) The quantification of the TRAP-positive osteoclasts on surfaces of AB at different time-points. The TRAP-positive osteoclasts were quantified and normalized by the length of the alveolar contour. (D) The quantification of the TRAP-positive osteoclasts on surfaces of CC. The number was normalized by the length of cementum contour. (E) Representative TRAP staining image of cementum resorption under high compression force. Resorption area was illustrated as a yellow translucent area. (F) Evaluation of root resorption. Root resorption scores=(the number of grids with resorption lacunae/the total number of grids along the root surface) x100. Scale bar, 50 μm. *P<0.05 compared between LF and HF at the same time-point; $^{\#}$P<0.05 compared with the control group. TRAP, tartrate-resistant acid phosphatase; ROI, region of interest; CC, cellular cementum; AB, alveolar bone; Ctrl, control; LF, low force; HF, high force; RA, resorption area; Oc, osteoclasts; PDL, periodontal ligament; ns, not significant.

alveolar bone demonstrated increased ratios over time. The increase in the *RANKL/OPG* ratio was higher in the cellular cementum than that of the alveolar bone from day 4.

Immunofluorescence staining of the cementocytes and osteocytes under compression conditions. Immunostaining of SOST protein was performed to assess its dynamic expression in the cellular cementum and the alveolar bone. SOST expression (labeled red) increased in osteocytes incubated under both low and high force conditions at days 4, 7 and 14 (Fig. 5A and D). In contrast to these findings, the cementocyte-like cells of the low force group exhibited a slightly increased SOST protein expression at day 4, and significant lower expression at days 7 and 14 compared to day 0, while those of the high force group exhibited an increased trend in SOST protein expression (Fig. 5B and C). The alveolar bone also exhibited an up-and down expression pattern, but the expression levels on days 7 and 14 were significantly higher than that on day 0. In the high force group, differences in sclerostin labelling between cementum and alveolar bone were not found to be associated with the force magnitude at any time-point. But in the low force group, higher SOST expression was detected on the compressive bone side compared to the tooth side at days 4, 7 and 14.

Discussion

The present study established a molar intrusion rat model and demonstrated that the cementocytes were sensitive to *in vivo* orthodontic force by inducing *SOST*, *OPG*, and *RANKL* expression. The results indicated that cementocytes contributed to the root protection during tooth intrusion under light force conditions, while under heavy orthodontic force conditions, the expression profiles of these markers in the cementocytes were altered.

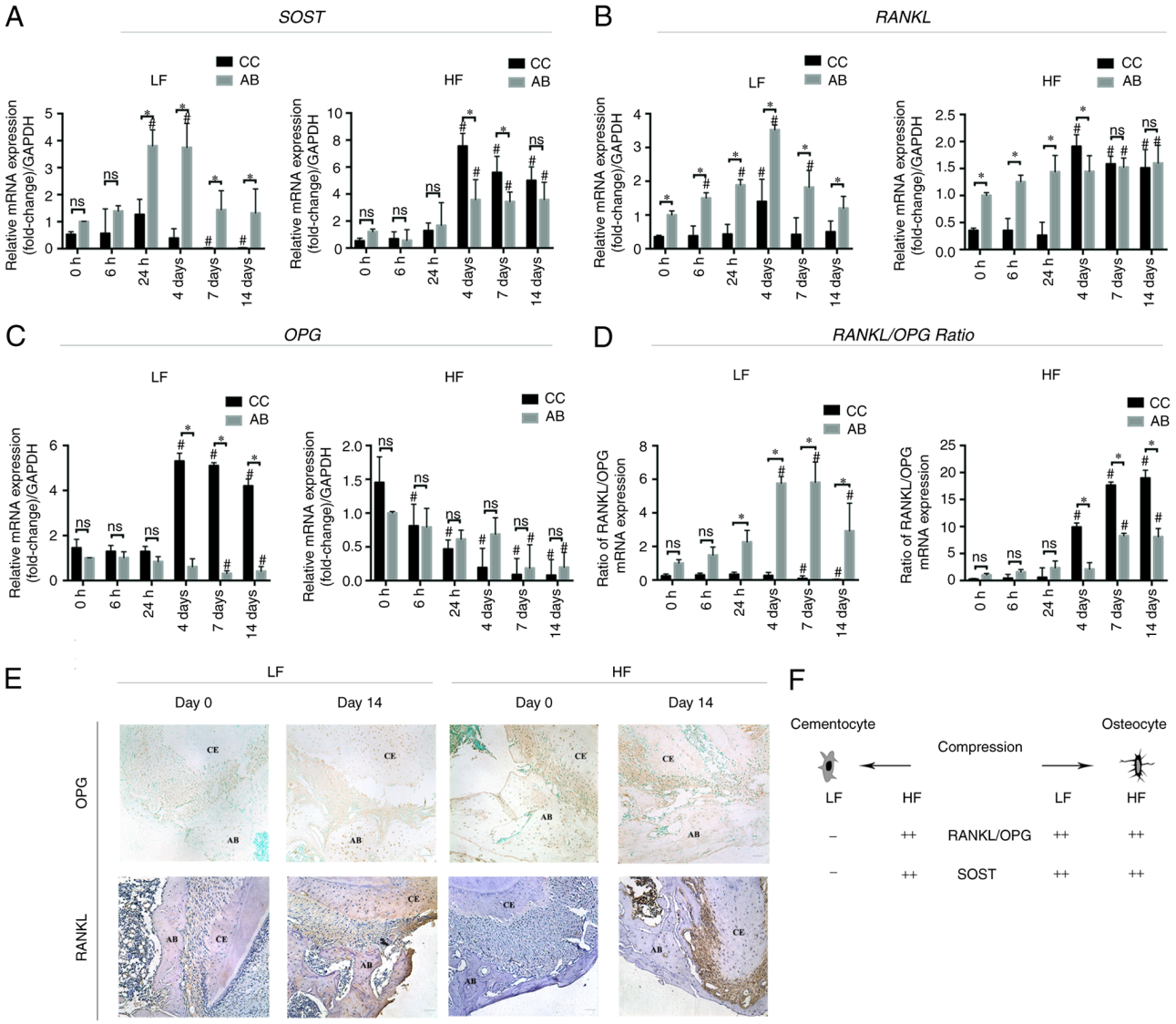

Figure 4. Reverse transcription-quantitative PCR analysis. (A) Relative *SOST* mRNA expression to *GAPDH* in the CC low and high force groups. AB was used for comparison. (B) Relative *RANKL* mRNA expression. (C) Relative *OPG* mRNA expression. (D) Relative ratio of *RANKL* and *OPG* mRNA expression. *P<0.05 compared between CC and AB at the same time-point; #P<0.05 compared with 0 h. (E) Immunohistochemical staining (magnification, x200) of OPG and RANKL. Scale bar, 50 μm. (F) Illustration of the changes of the expression profile of cementocytes and osteocytes under orthodontic compression force. *SOST*, sclerostin; CC, cellular cementum; AB, alveolar bone; *RANKL*, receptor activator of nuclear factor-κB ligand; *OPG*, osteoprotegerin; LF, low force; HF, high force; ns, not significant.

A limited number of studies have been performed to assess the biological behavior of the cementocytes following mechanical loading. Rodents are considered optimal experimental models since they possess similar anatomical features to that of humans (19). The direction of the orthodontic forces leads to alternative results. Odagaki *et al* (20) demonstrated a different pattern of SOST modulation on the tension and compression sides of the tooth movement. The mesial traction model of the rat molar is widely used. This model allows easy access to the simultaneous tension and compression force. However, since the molar is a multi-root irregular structure, the traction often leads to teeth tilting and uneven distribution of stress, notably on the root tip covered by the cellular cementum. Since the compression area is often associated with bone remodeling and root resorption, the current model was established in an attempt to apply compression forces with single direction and investigate the intrusion-induced tooth movement and the associated root resorption. The force direction was designed as parallel to the long axis of the tooth by the wire shape and position adjustment. μ-CT indicated tooth intrusion along the long axis of the tooth.

Force-induced tooth movement is initiated by instantaneous tooth movement within the socket (21), which is followed by strain induction in the matrix of the periodontal ligament (22) and a fluid flow shear stress in the cementum and bone tissue (23). The tissue strains and fluid flow stress are directly and indirectly transferred to the cells, activating a variety of signaling pathways, such as the integrin and the Wnt/b-catenin pathways, leading to mediator release and the activation of specific cells (24,25). Several markers which cementocytes express may play an important role in the process, including E11, which functions in dendrite development, DMP1, which is a secreted ECM phosphoprotein that may regulate mineralization, and sclerostin, which is a negative

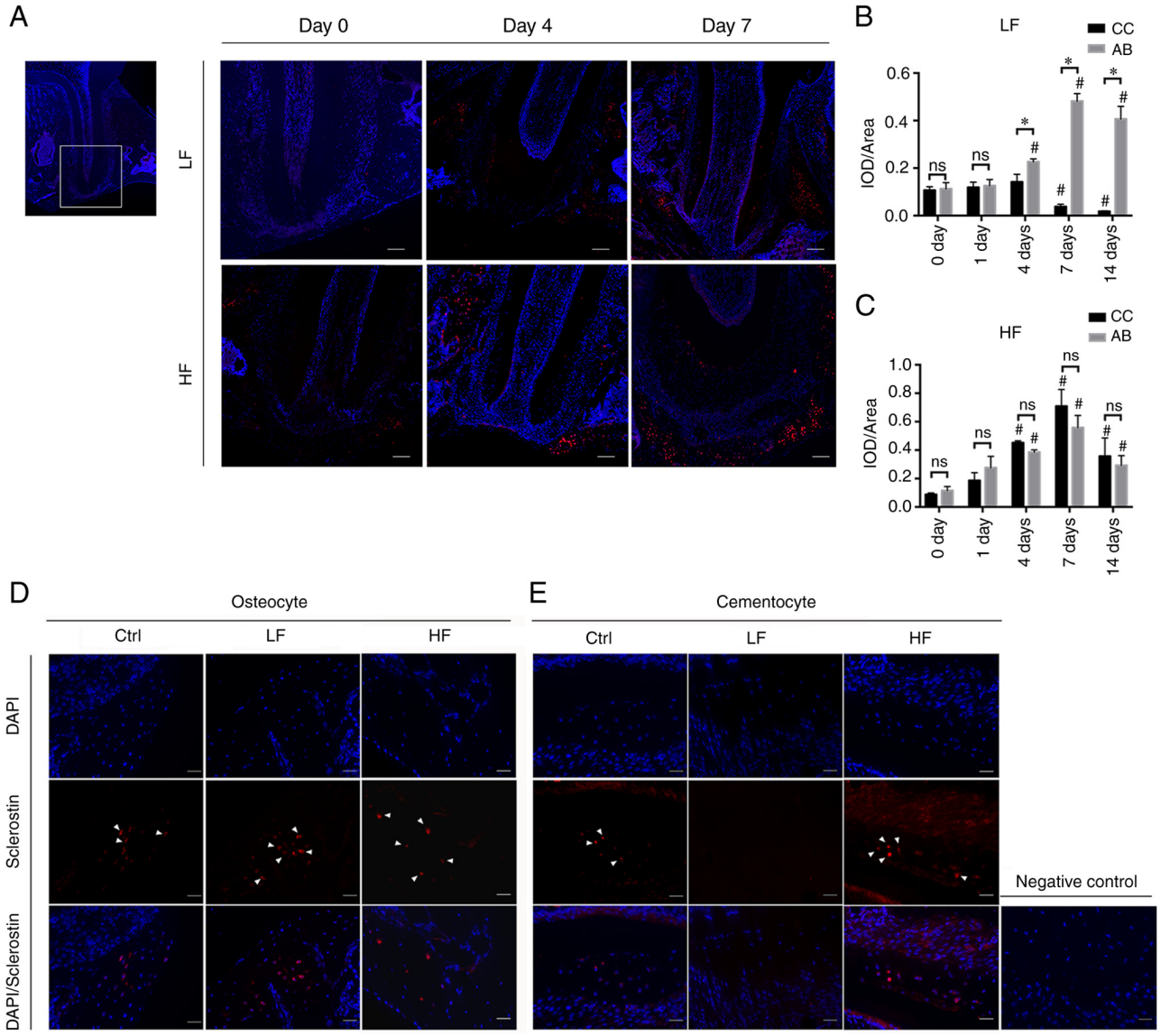

Figure 5. Immunostaining images of sclerostin. (A) representative images (magnification, x100) of the ROI, the mesial root of the left first molar on days 0, 4 and 7. Scale bar, 50 μm. (B and C) IOD value per area in the ROI region. The mean density of sclerostin labelling in the (B) light force group and (C) high force group were presented at each time-point. *P<0.05 compared between CC and AB at the same time-point; $^{\#}$P<0.05 compared with 0 days. (D) Immunostaining images (magnification, x400) of sclerostin on day 14. Sclerostin expression in the osteocytes in each group. The nuclei of osteocytes were labeled by DAPI (blue). Sclerostin was labeled red and indicated by white arrows. (E) Sclerostin (red) and DAPI (blue) immunostaining of the cementocytes (scale bar, 20 μm). The image on the right is the negative control. ROI, region of interest; IOD, integrated optical density; CC, cellular cementum; AB, alveolar bone; ns, not significant.

Wnt signaling regulator (26). A recent study has also demonstrated the roles and mechanisms of the YAP/TAZ pathway in the orthodontic force transduction. YAP and TAZ are capable of reading mechanical cues, such as shear stress, cell shape, and extracellular matrix rigidity, and stimulate downstream cellular activity (27).

The macrophage colony-stimulating factor family stimulates the osteoclast differentiation and RANKL binds to RANK on the osteoclast precursors initiating differentiation (28). OPG is the competitive antagonist of RANKL. The binding of OPG to RANK inhibits the terminal stage of osteoclast differentiation (29). SOST is a critical regulator of bone remodeling and metabolism and is a selective marker of mature osteocytes (30). SOST acts as an antagonist of lipoprotein receptor 5. Downregulation of the expression levels of *SOST* and Dickkopf WNT signaling pathway inhibitor 1 (*DKK1*) is essential for the release of the Wnt protein, which can activate the Wnt pathway (31). The expression profiles of these markers regulate the balance of osteoclast and osteoblast activation and differentiation. Osteocytes have been shown to express these cytokines and are considered key regulators of bone remodeling (32).

However, studies that have utilized cementocytes are limited. The results of the present study indicated that under light orthodontic forces, the cementocytes exhibited inhibitory effects on osteoclast differentiation (reduced recruitment of osteoclasts, downregulation of the expression levels of *SOST, RANKL*, and decreased *RANKL/OPG* ratio, upregulation of *OPG* mRNA levels and decrease in SOST protein expression). Reduced osteoclast activity on the surface of the cementum contributes to the homeostasis of the tooth root in the tooth movement. Moreover, the alveolar bone exhibited an increase

in osteoclastogenesis (higher level of osteoclast recruitment, increased *SOST* and *RANKL* expression levels, increased *RANKL*/*OPG* ratio and upregulation of *OPG* mRNA levels, all of which accelerated bone remodeling as demonstrated by μ-CT analysis). These findings may explain the continuous tooth movement by a relatively steady rate from day 0 to day 7.

Under light force conditions, osteoclast infiltration was detected at 6 h on the bone side and was significantly increased over time. Upregulation of *RANKL* expression in the alveolar bone was also detected after 6 h. It has been reported that in the early stage of osteoclast activation, recruitment of adaptor molecules, such as tumor necrosis factor receptor-associated factor 6, can mediate RANKL signaling and induce activation of mitogen-activated protein kinases, nuclear factor-κB and activator protein-1 (33). Induction of *RANKL* expression in the cementocytes was noted by light forces only on day 4. The temporal increase of the expression of this marker may be due to the stress change following tooth movement, the occlusal force interference, and a possible periodontal contamination. The relative ratio of *RANKL*/*OPG* is essential to maintain osteoclast differentiation, thereby playing a vital role in the regulation of bone remodeling (34). The results of the present study indicated that under light force conditions, the cellular cementum maintained steady levels of the *RANKL*/*OPG* ratio in the early stages, whereas a decrease was noted from days 7 to 14, which paralleled *SOST* expression, indicating an osteoclast inhibitory effect and a potential osteogenesis role in the early and late stages of mechanical loading, respectively.

Other studies have also reported the expression of these genes in the cementocytes. Jäger *et al* (35) demonstrated localized SOST expression in the cementocytes of mouse and human tissues. In addition, *SOST*-deficient mice indicated deposition of a thicker layer of the cellular cementum together with thicker alveolar bone (36), and increased mineral density (37). Cementocytes have also been reported to express RANKL in response to endodontic infection in mice (38).

Following the application of heavy forces on teeth, the expression profiles of both cementocytes and osteocytes were altered. Heavy forces induced higher *SOST* and *RANKL* expression levels, reduced *OPG* expression levels and higher *RANKL*/*OPG* ratio compared with the corresponding levels of these markers noted in osteocytes. The robust effect was initially detected on day 4 (*SOST* and *RANKL*). The expression levels noted in cementocytes were higher than those noted in the osteocytes, leading to a higher capacity of osteoclast induction by the cementocytes. This is a possible reason of root resorption. Furthermore, μ-CT demonstrated a sudden increase in tooth movement, indicating that the latter was a possible result of root resorption rather than bone remodeling. The extent of osteoclast quantification further indicated that the force magnitude did not increase the number of osteoclasts in the alveolar bone, while the increase of the force magnitude caused a significant increase in the osteoclast number on the cementum surfaces.

The magnitude of the applied force is usually considered directly proportional to osteoclastogenesis. Overloading leads to severe bone resorption, the development of pathological lesions in periodontal tissues, and external root resorption. Previous studies have reported that significant root resorption occurs with a loading ≥50 g compared with unloading or loading with 10 g (3). In addition, a 40-g force induces a higher level of cementocyte death (39). The results of the present study demonstrated that high force induced more bone remodeling, periodic tooth movement and more osteoclast distribution on the cementum side compared with the low force. Additional root resorption under high force due to the cementocyte behavior may be related to the small amount of cementocytes, the presence of micro-cracks in the matrix, the hypoxic environment, as well as the inflammatory conditions noted in the periodontal cells (40). Further investigations are required to verify these findings.

Periodontal cells have been demonstrated to play key roles in stimulating mechanotransduction (41,42). The contamination of periodontal cells may impact this process. In the present study, various efforts were made to avoid periodontal contamination. The tissues were dissected thoroughly in three cycles of serial digestion. The presented results paralleled with the *in vitro* study on cementocytes indicating that the mechanical loading altered the expression pattern of the cementocytes (6). However, the ability of the loading to affect the cells in a periodontal-dependent way requires further assessment. The crosstalk of periodontal cells and cementocytes should be investigated further.

Other limitations of the present study include lack of discussion regarding tension. As aforementioned, the cells may act differently following different force direction. Further investigations of the cellular response to different force types need to be performed.

In conclusion, the present study established an experimental tooth movement model by compressive loading and presented evidence that the cementocytes participate in the mechanotransduction pathway leading to tooth movement via modulation of the expression levels of *SOST, RANKL*, and *OPG*. High forces are not essential to accelerate tooth movement and induce more osteoclast differentiation on the surfaces of the cementum. The cementocytes act differently from the osteocytes by alternative expression patterns of cytokines, leading to different distribution of the activated osteoclasts when subjected to low force; therefore they play a protective role in tooth root homeostasis. Excessive forces may alter this role and induce higher levels of osteoclast differentiation. Further investigations, such as the use of gene profiling can potentially provide relevant targets focusing on the biochemical and biomechanical roles of the cementocytes. These targets can be exploited therapeutically for tooth root protection and regeneration therapy. These findings add to our understanding of the biological mechanisms of the force-induced tooth movement.

Acknowledgements

The authors would like to thank Dr Quan Yu (Shanghai Ninth People's Hospital, Shanghai Jiao Tong University School of Medicine, Shanghai, China) for advice on methodology and visualization. The authors would also like to thank Dr Zhifeng Yu (Shanghai Ninth People's Hospital, Shanghai Jiao Tong University School of Medicine, Shanghai, China) for guidance on micro-computed tomography scanning.

Funding

The present study was funded by the National Natural Science Foundation of China (grant nos. 81771104 and 82171011).

Availability of data and materials

The datasets used and/or analyzed in the present study are available from the corresponding author on reasonable request.

Authors' contributions

TW performed the experiments and drafted the manuscript. ZS contributed to data analysis and interpretation, and critically revised the manuscript. XW contributed to the statistical analysis and drafted the manuscript. NZ contributed to the conception of the study and interpretation of the data, and critically revised the manuscript. GS contributed to the conception and design of the study, and critically revised the manuscript. NZ and GS confirm the authenticity of the raw data. All authors have read and approved the final version of the manuscript.

Ethics approval and consent to participate

The animal experiments were approved (approval no. SH9H-2020-A298-1) by the Animal Ethics Committee of Shanghai Ninth People's Hospital (Shanghai, China).

Patient consent for publication

Not applicable.

Competing interests

The authors declare that they have no competing interests.

References

1. Feller L, Khammissa RA, Thomadakis G, Fourie J and Lemmer J: Apical external root resorption and repair in orthodontic tooth movement: Biological events. Biomed Res Int 2016: 4864195, 2016.
2. Ozkalayci N, Karadeniz EI, Elekdag-Turk S, Turk T, Cheng LL and Darendeliler MA: Effect of continuous versus intermittent orthodontic forces on root resorption: A microcomputed tomography study. Angle Orthod 88: 733-739, 2018.
3. Gonzales C, Hotokezaka H, Yoshimatsu M, Yozgatian JH, Darendeliler MA and Yoshida N: Force magnitude and duration effects on amount of tooth movement and root resorption in the rat molar. Angle Orthod 78: 502-509, 2008.
4. Ueda M, Kuroishi KN, Gunjigake KK, Ikeda E and Kawamoto T: Expression of SOST/sclerostin in compressed periodontal ligament cells. J Dent Sci 11: 272-278, 2016.
5. Li Y, Zhan Q, Bao M, Yi J and Li Y: Biomechanical and biological responses of periodontium in orthodontic tooth movement: Up-date in a new decade. Int J Oral Sci 13: 20, 2021.
6. Wei T, Xie Y, Wen X, Zhao N and Shen G: Establishment of in vitro three-dimensional cementocyte differentiation scaffolds to study orthodontic root resorption. Exp Ther Med 20: 3174-3184, 2020.
7. Lira Dos Santos EJ, de Almeida AB, Chavez MB, Salmon CR, Mofatto LS, Camara-Souza MB, Tan MH, Kolli TN, Mohamed FF, Chu EY, *et al*: Orthodontic tooth movement alters cementocyte ultrastructure and cellular cementum proteome signature. Bone 153: 116139, 2021.
8. Lira Dos Santos EJ, Salmon CR, Chavez MB, de Almeida AB, Tan MH, Chu EY, Sallum EA, Casati MZ, Ruiz KGS, Kantovitz KR, *et al*: Cementocyte alterations associated with experimentally induced cellular cementum apposition in Hyp mice. J Periodontol 92: 116-127, 2021.
9. Krishnan V and Davidovitch Z: On a path to unfolding the biological mechanisms of orthodontic tooth movement. J Dent Res 88: 597-608, 2009.
10. Borges de Castilhos B, Machado de Souza C, Simas Netta Fontana ML, Pereira FA, Tanaka OM and Trevilatto PC: Association of clinical variables and polymorphisms in RANKL, RANK, and OPG genes with external apical root resorption. Am J Orthod Dentofacial Orthop 155: 529-542, 2019.
11. Weivoda MM, Youssef SJ and Oursler MJ: Sclerostin expression and functions beyond the osteocyte. Bone 96: 45-50, 2017.
12. Lim WH, Liu B, Hunter DJ, Cheng D, Mah SJ and Helms JA: Downregulation of Wnt causes root resorption. Am J Orthod Dentofacial Orthop 146: 337-345, 2014.
13. Underwood W and Anthony R: AVMA Guidelines for the Euthanasia of Animals. American Veterinary Medical Association, Schaumburg, 2020.
14. Gonzales C, Hotokezaka H, Arai Y, Ninomiya T, Tominaga J, Jang I, Hotokezaka Y, Tanaka M and Yoshida N: An in vivo 3D micro-CT evaluation of tooth movement after the application of different force magnitudes in rat molar. Angle Orthod 79: 703-714, 2009.
15. Wolf M, Ao M, Chavez MB, Kolli TN, Thumbigere-Math V, Becker K, Chu EY, Jäger A, Somerman MJ and Foster BL: Reduced orthodontic tooth movement in Enpp1 mutant mice with hypercementosis. J Dent Res 97: 937-945, 2018.
16. Lu LH, Lee K, Imoto S, Kyomen S and Tanne K: Histological and histochemical quantification of root resorption incident to the application of intrusive force to rat molars. Eur J Orthod 21: 57-63, 1999.
17. Zhao N, Nociti FH Jr, Duan P, Prideaux M, Zhao H, Foster BL, Somerman MJ and Bonewald LF: Isolation and functional analysis of an immortalized murine cementocyte cell line, IDG-CM6. J Bone Miner Res 31: 430-442, 2016.
18. Livak KJ and Schmittgen TD: Analysis of relative gene expression data using real-time quantitative PCR and the 2(-Delta Delta C(T)) method. Methods 25: 402-408, 2001.
19. Yamamoto T, Domon T, Takahashi S, Islam MN and Suzuki R: The fibrillar structure of cementum and dentin at the cemento-dentinal junction in rat molars. Ann Anat 182: 499-503, 2000.
20. Odagaki N, Ishihara Y, Wang Z, Ei Hsu Hlaing E, Nakamura M, Hoshijima M, Hayano S, Kawanabe N and Kamioka H: Role of osteocyte-PDL crosstalk in tooth movement via SOST/Sclerostin. J Dent Res 97: 1374-1382, 2018.
21. Rygh P: Ultrastructural changes in pressure zones of human periodontium incident to orthodontic tooth movement. Acta Odontol Scand 31: 109-122, 1973.
22. Binderman I, Bahar H and Yaffe A: Strain relaxation of fibroblasts in the marginal periodontium is the common trigger for alveolar bone resorption: A novel hypothesis. J Periodontol 73: 1210-1215, 2002.
23. Harter LV, Hruska KA and Duncan RL: Human osteoblast-like cells respond to mechanical strain with increased bone matrix protein production independent of hormonal regulation. Endocrinology 136: 528-535, 1995.
24. Du Y, Ling J, Wei X, Ning Y, Xie N, Gu H and Yang F: Wnt/β-catenin signaling participates in cementoblast/osteoblast differentiation of dental follicle cells. Connect Tissue Res 53: 390-397, 2012.
25. Goldmann WH: Mechanical aspects of cell shape regulation and signaling. Cell Biol Int 26: 313-317, 2002.
26. Zhao N, Foster BL and Bonewald LF: The cementocyte-an osteocyte relative?. J Dent Res 95: 734-741, 2016.
27. Deng L, Chen Y, Guo J, Han X and Guo Y: Roles and mechanisms of YAP/TAZ in orthodontic tooth movement. J Cell Physiol 236: 7792-7800, 2021.
28. Nakano Y, Yamaguchi M, Fujita S, Asano M, Saito K and Kasai K: Expressions of RANKL/RANK and M-CSF/c-fms in root resorption lacunae in rat molar by heavy orthodontic force. Eur J Orthod 33: 335-343, 2011.
29. Silva I and Branco JC: Rank/Rankl/opg: Literature review. Acta Reumatol Port 36: 209-218, 2011.
30. Boyle WJ, Simonet WS and Lacey DL: Osteoclast differentiation and activation. Nature 423: 337-342, 2003.
31. Liu M, Kurimoto P, Zhang J, Niu QT, Stolina M, Dechow PC, Feng JQ, Hesterman J, Silva MD, Ominsky MS, *et al*: Sclerostin and DKK1 inhibition preserves and augments alveolar bone volume and architecture in rats with alveolar bone loss. J Dent Res 97: 1031-1038, 2018.
32. Bonewald LF: The amazing osteocyte. J Bone Miner Res 26: 229-238, 2011.
33. Park JH, Lee NK and Lee SY: Current understanding of RANK signaling in osteoclast differentiation and maturation. Mol Cells 40: 706-713, 2017.

34. Yamaguchi M: RANK/RANKL/OPG during orthodontic tooth movement. Orthod Craniofac Res 12: 113-119, 2009.
35. Jäger A, Götz W, Lossdörfer S and Rath-Deschner B: Localization of SOST/sclerostin in cementocytes in vivo and in mineralizing periodontal ligament cells in vitro. J Periodontal Res 45: 246-254, 2010.
36. Kuchler U, Schwarze UY, Dobsak T, Heimel P, Bosshardt DD, Kneissel M and Gruber R: Dental and periodontal phenotype in sclerostin knockout mice. Int J Oral Sci 6: 70-76, 2014.
37. Li X, Ominsky MS, Niu QT, Sun N, Daugherty B, D'Agostin D, Kurahara C, Gao Y, Cao J, Gong J, *et al*: Targeted deletion of the sclerostin gene in mice results in increased bone formation and bone strength. J Bone Miner Res 23: 860-869, 2008.
38. De Rossi A, Fukada SY, De Rossi M, da Silva RA, Queiroz AM, Nelson-Filho P and da Silva LA: Cementocytes express receptor activator of the nuclear factor Kappa-B ligand in response to endodontic infection in mice. J Endod 42: 1251-1257, 2016.
39. Matsuzawa H, Toriya N, Nakao Y, Konno-Nagasaka M, Arakawa T, Okayama M and Mizoguchi I: Cementocyte cell death occurs in rat cellular cementum during orthodontic tooth movement. Angle Orthod 87: 416-422, 2017.
40. Diercke K, Kohl A, Lux CJ and Erber R: Compression of human primary cementoblasts leads to apoptosis: A possible cause of dental root resorption? J OrofacOrthop 75: 430-445, 2014.
41. Lee SY, Moon JS, Yang DW, Yoo HI, Jung JY, Kim OS, Kim MS, Koh JT, Chung HJ and Kim SH: SLPI in periodontal Ligament is not sleepy during biophysical force-induced tooth movement. J Clin Periodontol 48: 528-540, 2021.
42. Moon JS, Lee SY, Kim JH, Choi YH, Yang DW, Kang JH, Ko HM, Cho JH, Koh JT, Kim WJ, *et al*: Synergistic alveolar bone resorption by diabetic advanced glycation end products and mechanical forces. J Periodontol 90: 1457-1469, 2019.